JOURNAL OF MATERIALS SCIENCE 31 (1996) 1815–1820

Elastic modulus and vibration damping in Iron/Copper- and steel-based metal matrix composites

A. WOLFENDEN, M. JACKSON
Mechanical Engineering Department, Texas A&M University, College Station, TX 77843, USA
N. MARTIROSIAN
Ave. Teryan, 19, Fl. 39, Yerevan, 375010, Armenia

Measurements were made of the dynamic flexural modulus, dynamic Young's modulus, damping, strain amplitude, and the strain amplitude dependence of damping in iron/copper- and steel-based metal matrix composites. Comparisons were made concerning the steel matrix specimens before and after heat treatment. The flexural modulus tests were performed using the Grindosonic technique, while the Young's modulus, damping, strain amplitude, and the strain amplitude dependence of damping were determined using the piezoelectric ultrasonic composite oscillator technique (PUCOT). Metallographic studies utilizing chemical etching, optical and electron microscopy, and microhardness testing were performed to assess the distribution of the fibres in the composites. The variation of dynamic Young's modulus with respect to percentage copper in the composites followed the rule of mixtures.

1. Introduction

In many applications, metal matrix composites (MMCs) are preferred to pure metals, due to the fact that the mechanical properties of composites can be controlled to a greater degree. These properties may be influenced by the manufacturer's choice of alloying elements and fibre orientation. Advanced composites can provide some unusually attractive features. These include simultaneous increases in thermal conductivity, strength, and elastic modulus with judicious choices of matrices and fibres. We concentrate here only on the mechanical properties and microstructure of iron/copper- and steel-based MMCs, working with the premise that the presence of copper in iron or steel will increase the electrical and thermal conductivities. The matter of concern is whether the promotion of the conductivities is at the expense of significant loss of stiffness. In two of the specimens, fibres of molybdenum (whose elastic modulus is greater than that of iron or steel) were incorporated, along with the increased percentage of copper, to offset the anticipated reduction in stiffness (due to copper) of the MMC.

2. Experimental procedure

The metal matrix composite specimens tested are listed in Table I.

The specimens were prepared from powders of the appropriate compositions and chopped fibres, using standard methods of powder metallurgy, followed by extrusion. Other aspects of the manufacturing process are proprietary.

Measurements of dynamic Young's modulus, damping, strain amplitude, and the strain amplitude dependence of damping for each specimen were obtained using the piezoelectric ultrasonic composite oscillator technique (PUCOT). Additional information concerning the PUCOT may be found elsewhere [1]. Each specimen was sectioned using an Isomet 11-1180 low-speed saw. The PUCOT used was a solid-state equipment closed-loop crystal driver together with 80 kHz (longitudinal) quartz crystals.

Heat treatment was performed on the steel matrix specimens using Sybron Thermolyne closed furnaces in order that the elastic modulus and strain amplitude dependence of damping after heat treating could be compared with the initial data and any possible changes in microstructure could be assessed. To facilitate this assessment, metallographic studies were performed on each composite specimen. Longitudinal and transverse sections of each specimen were mounted in bakelite using a Buehler Simplimet II mould press. Following mounting, the specimens were polished using Buehler Ecomet II polishing wheels. The mounted composite specimens were analysed using a Nikon Epiphot-TME inverted microscope and a JEOL 6400 scanning electron microscope. Since some specimens exhibited multiple phases,

0022–2461

TABLE I MMC specimens tested

Specimen number	Matrix	Fibre	
1	Fe(75%) + Cu(15%)	Mo(10%)	$L/d = 50$
2	Fe(75%) + Cu(15%)	Mo(10%)	$L/d = 150$
3	Fe(55%) + Cu(15%)	Steel(30%)	$L/d = 150$
4	Steel(Fe + 0.45% C)	Cu(10%)	$L/d = 150$
5	Steel(Fe + 0.45% C)	Cu(30%)	$L/d = 150$

L: Specimen length; d: diameter

microhardness tests were performed using a Buehler Micromet II digital microhardness tester.

The mass density (ρ) of each specimen was determined in two ways. First, the mass (m) of each specimen in air was measured using the balance. The dimensions of each specimen were measured and the volume (V) calculated. The density of each specimen was then determined using the following equation:

$$\rho = m/V \quad (1)$$

Additional density values were obtained by measuring the mass of each specimen in air, the mass of each specimen suspended in distilled water by a copper wire, and the mass of the wire. The density data obtained from each method was then assessed using the rule of mixtures.

Following density calculations, the flexural modulus of each composite specimen was determined using the Grindosonic technique in a manner similar to that employed by Heritage *et al.* [2]. Each specimen was supported above a microphone attached to the Grindosonic machine and at points approximately one quarter of the specimen length from each end. When the centre of the specimen was struck ballistically with a small metal rod (approximately 3 mm in diameter), the machine recorded a number (Gr) that was converted into a resonant frequency (f) according to the equation

$$f = 32 \times 10^6/Gr \quad (2)$$

Using a correction factor (T) provided by Spinner and Tefft [3] and based on Poisson's ratio and the diameter/length (d/L) ratio of the specimen, the flexural modulus (E) of the specimen was calculated according to the equation

$$E = 1.261886\ (\rho)\ (L^4)\ (f^2)\ (T)/d^2 \quad (3)$$

The flexural modulus data were then assessed with the rule of mixtures.

The elastic modulus, damping, strain amplitude, and strain amplitude dependence of each composite specimen were determined using the piezoelectric ultrasonic composite oscillator technique (PUCOT). The PUCOT involved the end-to-end mounting of the specimen to an 80 kHz (longitudinal) crystal using Loctite glue. The crystal itself was connected to alumel wires with silver paint. The wires in turn were connected to a solid-state equipment closed-loop crystal driver through drive and gauge voltage leads. The crystal driver was adjusted so that the combined crystals and specimen resonated at approximately the period of the crystals and the drive and gauge voltages were recorded.

These voltage values, together with the specimen density, period of the crystals, mass of the crystals, length and mass of the specimen, and the period of the combined crystals and specimen were used to determine the elastic modulus, damping, and strain amplitude of each specimen.

The strain amplitude dependence of damping was determined by obtaining data for gauge voltage values of 0.003, 0.01, 0.03, 0.1, 0.3, 1 and 3 V. Damping was then plotted against strain amplitude from these data. Strain amplitudes in the range 10^{-7} to 10^{-4} were explored.

It was desired to compare data for the steel matrix specimens (4 and 5) before and after heat treatment. Sections of both specimens were hardened for 30 min at 860 °C, quenched in water, and tempered at 200 °C for 1 h. PUCOT measurements were then repeated for the two heat-treated specimens.

Using the data gathered in the PUCOT tests, an analysis was made of two representative specimens using the Granato–Luecke theory concerning vibrating dislocations within a material [4, 5]. Minor pinning lengths and mobile dislocation densities were calculated based on the damping and strain amplitude data, lattice parameter for iron [6], specimen density, dislocation network length and Burgers vector.

After the PUCOT tests were completed, each composite (including the two heat treated specimens) was mounted in bakelite for metallographic studies. The mounted specimens were then polished and examined under a Nikon Epiphot-TME inverted microscope. Microhardness tests were performed on those specimens exhibiting multiple phases using a Buehler Micromet II digital microhardness tester. Specimens 1, 2 and 3 were tested under a 500 g load and specimens 4 and 5 were tested under a 200 g load, all for 15 s. Following microhardness testing, both the steel matrix and the copper fibres were studied through chemical etching and re-examined using optical microscopy. Final microstructural analysis was performed using a scanning electron microscope, which yielded informative data through X-ray analysis.

3. Results and discussion

Both methods of density determination agree fairly well, but the Archimedes method is regarded as the more precise (see Table II). For this reason, the

TABLE II Density measurements

Specimen number	Density (g cm^{-3})			
	Dimensional method	Archimedes method, A	Rule of mixtures, R	$V_p[(A-R)/A]$ (%)
1	8.23	8.23	8.27	− 0.49
2	8.20	8.22	8.27	− 0.61
3	7.90	7.86	8.04	− 2.29
4	7.66	7.69	7.98	− 3.77
5	7.88	7.93	8.20	− 3.40

TABLE III Data for elastic modulus, strain amplitude and damping

Specimen number	E_{Grindo}[b] (GPa)	E_{PUCOT}[c] (GPa)	Strain amplitude	Damping (Q^{-1})	R_c^d (GPa)
1	203.4	200.8	3.5×10^{-7}	2.3×10^{-4}	194.4
2	195.4	195.7	3.7×10^{-7}	1.7×10^{-4}	193.9
3	204.7	204.7	3.5×10^{-7}	1.1×10^{-4}	175.1
4	194.9	200.9	3.5×10^{-7}	2.3×10^{-4}	173.6
5	186.0	185.5	3.6×10^{-7}	2.7×10^{-4}	158.9
4-HT[a]	–	181.9	7.2×10^{-7}	6.5×10^{-4}	–
5-HT[a]	–	176.4	7.3×10^{-7}	1.5×10^{-3}	–

[a] HT: Heat treated.
[b] E_{Grindo}: Flexural modulus using Grindosonic technique.
[c] E_{PUCOT}: Young's modulus using PUCOT.
[d] R_c: Rule of mixtures corrected for porosity.
($R_c = R(1 - 2V_p - 0.5V_p^2)$, where R is rule of mixtures value of modulus.)

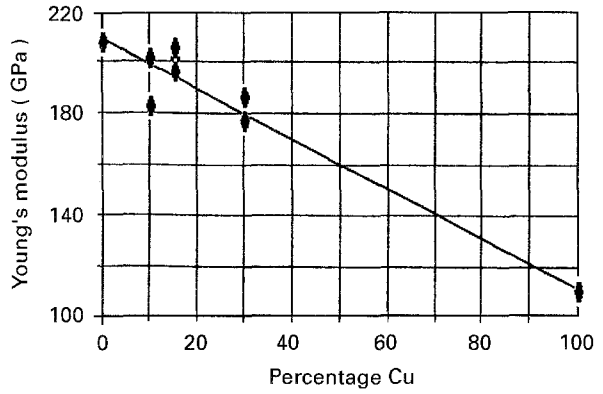

Figure 1 Dynamic Young's modulus versus percentage Cu.

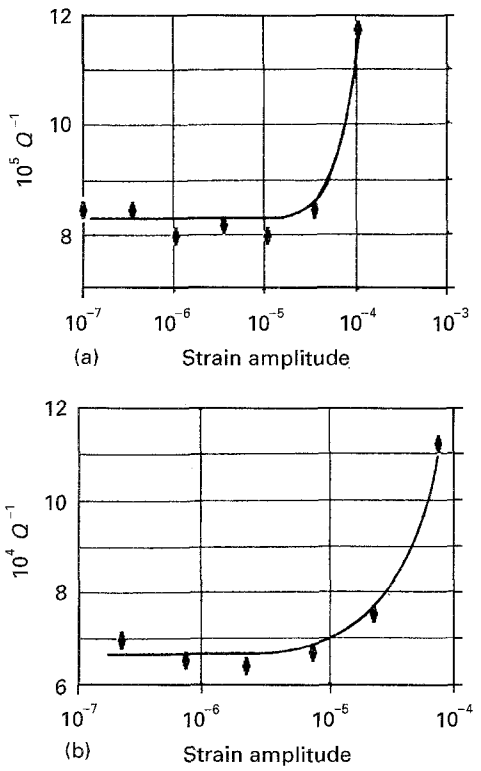

Figure 2 (a) Strain amplitude dependence of damping for specimen 3 55%Fe + 15%Cu matrix, 30% steel fibre ($L/d = 150$). (b) Strain amplitude dependence of damping for specimen 4-HT steel (Fe + 0.45%C) matrix, 10%Cu fibre ($L/d = 150$), heat treated.

Archimedes values were used in related calculations involving density. The agreement between the rule of mixtures data and the dimensional and Archimedes methods is not as close for specimens 3, 4, and 5 as it is for specimens 1 and 2. This could be the result of greater porosity in specimens 3 through to 5.

It should be noted from Table III that the Young's modulus data agree quite closely with the flexural modulus data obtained with the Grindosonic. Agreement between these two values suggests the lack of elastic anisotropy in the metal matrix composites. Specimens 1 and 2 have L/d ratios of 50 and 150, respectively. This difference in L/d ratio has little effect on either the flexural or Young's modulus values. The two heat-treated specimens also show a reduction in Young's modulus, and sharp increases in damping.

The dependence of the elastic modulus on the percentage of copper present in each specimen is shown in Fig. 1. The data points for pure iron (0% copper) and pure copper (100% copper) are taken as 207 and 110 GPa, respectively. The rule of mixtures line connects these two extrema and all data points have been curve-fitted. The trend of the curve is expected: as copper is added, the elastic modulus decreases and obeys the rule of mixtures. There should be no large changes in Young's modulus due to heat treatment of the MMCs unless there is generation of new, stiff phases in significant quantities (e.g. carbides). This is not likely to be the case in the low carbon (0.45% C) steel, and this is confirmed by the good fit (correlation coefficient $= -0.96$) of the data points to the curve.

The strain amplitude dependence of damping for specimen 3 and specimen 4-HT (heat treated) can be seen in Fig. 2a and b. All specimens showed relatively constant damping for strain amplitudes up to 1.0×10^{-5}. Above this strain amplitude, the damping increased rather rapidly. This behaviour suggests that dislocation damping occurs in the composites.

The damping data for specimens 3 and 4-HT were analyzed in terms of the Granato-Luecke theory of dislocation damping and the results are shown in Table IV. The minor pinning length gives the distance between the minor pinning points of the dislocations within the composite. The dislocation density

TABLE IV Granato–Luecke analysis

Specimen number	Minor pinning length (nm)	Mobile dislocation density (m^{-2})
3	8	2.0×10^{14}
4-HT	13	4.9×10^{15}

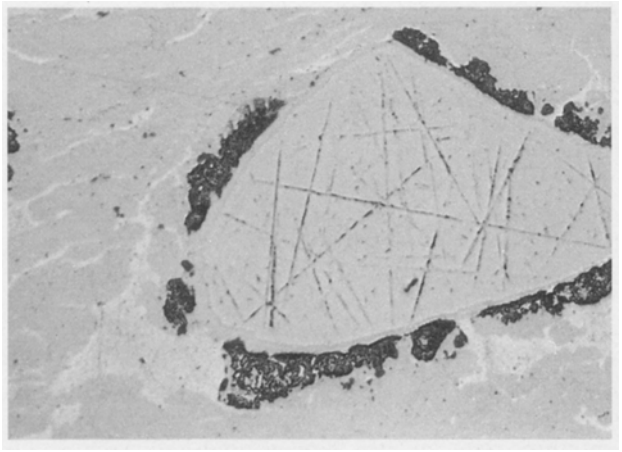

Figure 3 Longitudinal view of composite specimen number 2 (100×).

Figure 4 Longitudinal view of composite specimen number 3 (12.5×)

Figure 5 Longitudinal view of composite specimen number 5 (12.5×)

represents the number of mobile dislocations within the specimen. Such calculations should be regarded as order-of-magnitude calculations only, in view of the

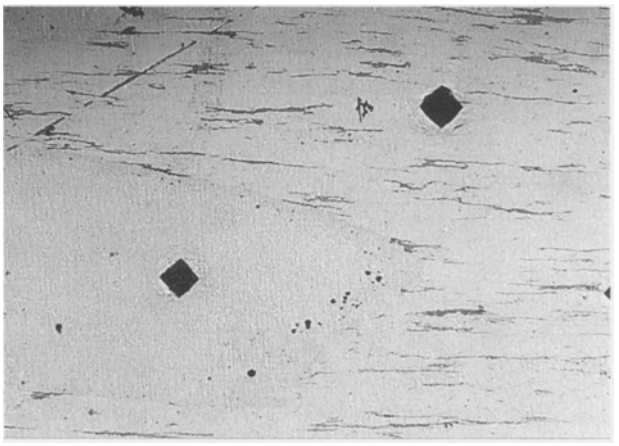

Figure 6 Microhardness test of composite specimen number 3 (25.25×): steel fibre (oval-shaped), 145 Hv; matrix (background), 109 Hv.

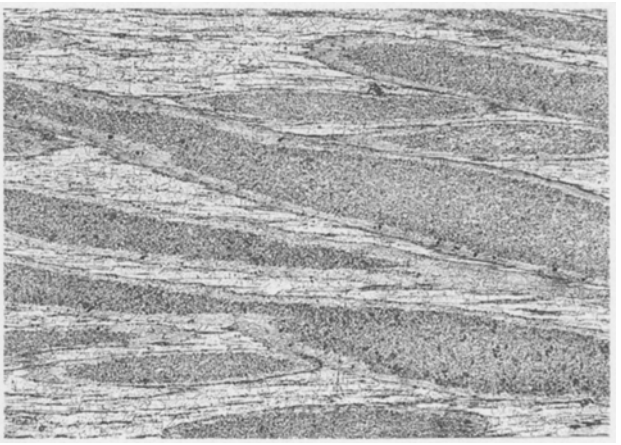

Figure 7 Longitudinal view of composite specimen number 3 (12.5×). (Etchant: 120 ml methanol, 30 ml HCl, 10 g iron (III) chloride.)

several assumptions incorporated. The values of dislocation density calculated here are rather high for materials that have seen high temperatures (either during processing or heat treatment) but are comparable with those calculated by Hartman *et al.* [7] for SiC/Al alloy metal matrix composites. An explanation of the high dislocation densities has been put forward by Arsenault and Fisher [8] in terms of the generation of dislocations at the fibre/matrix interfaces due to thermal stresses during cooling. It should be noted that the minor pinning lengths (Table IV) are smaller than the typical interfibre spacing in these composites. Therefore, the pinning involves impurities or species other than the fibres.

Photographs representing the results of the metallographic studies can be seen in Figs 3 through to 8. Fig. 3 is a close-up view of the grey phases found in specimens 1 and 2. The X-ray analysis performed with the scanning electron microscope (SEM) identified these phases as molybdenum fibres (Figs 9 and 10), which is consistent with the original description of the specimens. Since scratches appeared (during the polishing process) in the fibres and not in the matrix and the fibres were found (through microhardness testing) to be harder, it was assumed that they protruded from

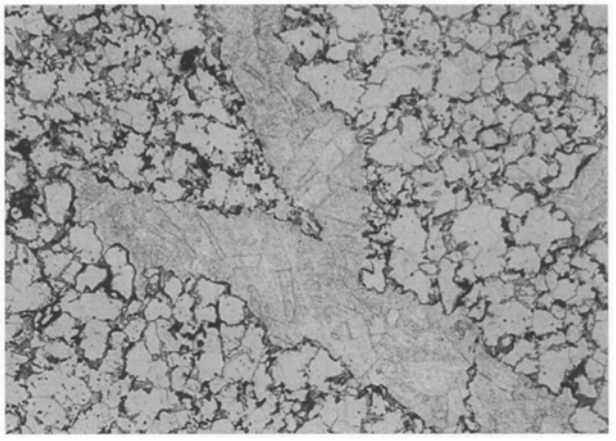

Figure 8 Transverse view of composite specimen number 4 (100 ×). (Etchant: 120 ml methanol, 30 ml HCl, 10 g iron (III) chloride.)

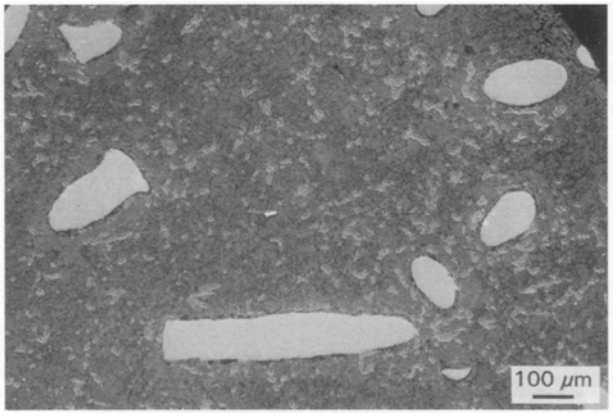

Figure 9 Longitudinal view of composite specimen number 2 (SEM).

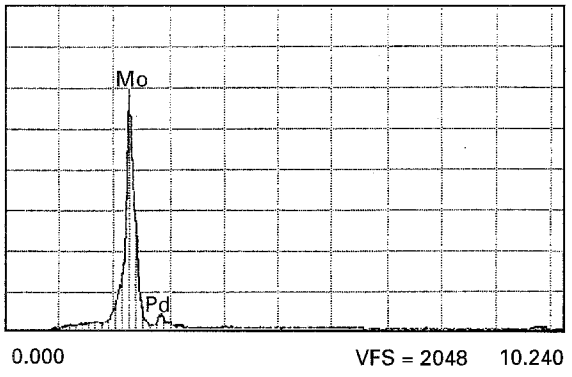

Figure 10 X-ray analysis of Mo fibre in specimen number 2.

the matrix. This assumption was confirmed by the SEM analysis. The linear streaks areas shown in Figs 3, 4, and 6 show the copper present in the matrices of the iron/copper-based specimens.

Fig. 4 shows the grey oval-shaped areas found in specimen 3 where the copper fibres seem to end. Microhardnesss tests (Fig. 6 and Table V) showed only a small difference in hardness between these oval-shaped areas (145 Hv) and the surrounding matrix (109 Hv). When the matrix (known to be steel) was chemically etched, these oval-shaped areas etched similarly to the matrix (Fig. 7). These findings, coupled

TABLE V Vickers microhardness for fibres and matrix

	Molybdenum Fibre (Hv)	Matrix (Hv)
Specimen 1	243	119
Specimen 2	256	116
	Steel Fibre (Hv)	Matrix (Hv)
Specimen 3	145	109
	Copper Fibre (Hv)	Matrix (Hv)
Specimen 4	97	173
Specimen 5	80	105

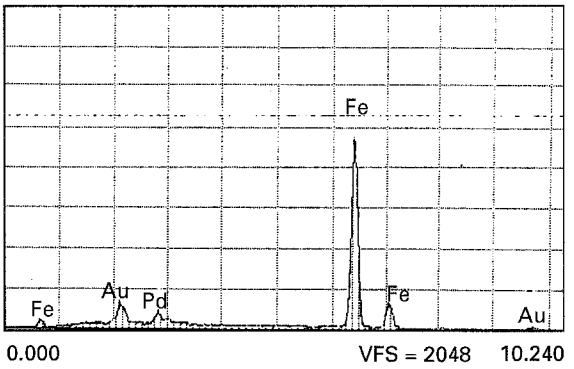

Figure 11 X-ray analysis of steel fibre in specimen number 3.

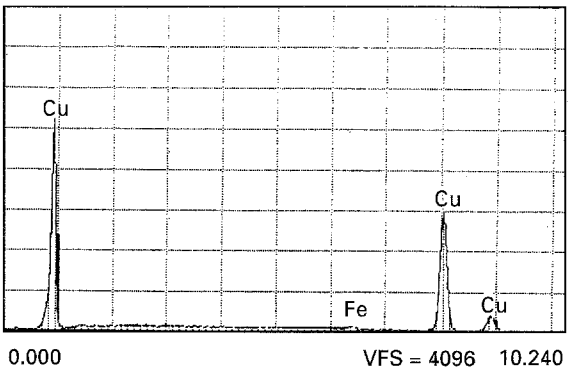

Figure 12 X-ray analysis of Cu fibre in specimen number 5.

with positive identification of the chemical make-up of the oval-shaped areas through SEM X-ray analysis (Fig. 11), proved them to be the expected steel fibres.

Figs 5 and 8 show the streaky copper fibres present in specimens 4 and 5. Fig. 5 shows the alignment of the fibres in the longitudinal direction due to extrusion, while the cross-sectional randomness of the fibres can be seen in Fig. 8, which shows the specimen after etching. Twinning in the copper fibres is also evident in this figure. X-ray analysis showed these fibres to be copper (Fig. 12) and the black areas appearing in some of the specimens to be mostly carbon (possibly appearing as a result of the steel production), with various other minor impurities.

4. Summary and conclusions

From an analysis of the various tests performed on the metal matrix composite specimens, the following conclusions can be made. On the microscopic level, the fibres in specimens 1 and 2 were confirmed to be molybdenum, the fibres in specimen 3 steel, and the

fibres in specimens 4 and 5 copper. The data obtained for both flexural modulus (using the Grindosonic technique) and Young's modulus (using the PUCOT) ranged from 186 to 205 GPa. The agreement between the particular values of elastic modulus obtained by the two measuring techniques suggests that the composite specimens are elastically isotropic. The strain amplitude dependence of damping in the specimens suggests that dislocation damping occurs within some of the composites. Additionally, heat treatment led to decreased Young's modulus (201 to 182 GPa, and 186 to 176 GPa) and increased damping. While it can be assumed that electrical and thermal conductivity are increased through the inclusion of the copper fibres, a decrease of up to 14% in Young's modulus was observed experimentally. Such a decrease in Young's modulus is relatively small and should not compromise the attractiveness of a material that combines high stiffness with improved electrical and thermal conductivities.

Acknowledgements

The authors thank the following for their valuable discussions, assistance, and continuous support: Drs R. Goforth, M. Coy, and M. Srinivasan, and S. Cronauer.

References

1. A. WOLFENDEN, M. R. HARMOUCHE, G. V. BLESSING, Y. T. CHEN, P. TERRANOVA, V. DAYAL, V. K. KINRA, J. W. LEMMENS, R. R. PHILLIPS, J. S. SMITH, P. MAHMOODI and R. J. WANN, *J. Testing Evaluation*, **17** (1989).
2. K. HERITAGE, C. FRISBY and A. WOLFENDEN, *Rev. Sci. Instrum.* **59** (1988) 973.
3. S. SPINNER and W. E. TEFFT, *Proc. ASTM* **61** (1961) 1230.
4. A. V. GRANATO and K. LUECKE, *J. Appl. Phys.* **27** (1956) 583.
5. *Idem, ibid.* **27** (1956) 789.
6. L. H. VAN VLACK, "Elements of Materials Science", 2nd Edn (Adisson-Wesley Publishing Co., Reading, Mass., 1964) p. 555.
7. J. T. HARTMAN Jr, K. H. KEENE, R. J. ARMSTRONG and A. WOLFENDEN, *J Metals* April (1986) 33.
8. R. J. ARSENAULT and R. M. FISHER, *Scripta Metall.* **17** (1983) 67.

Received 8 February 1994
and accepted 7 June 1995